

Direct Power Control of Brushless Doubly-fed Induction Generator Used in Wind Energy Conversion System

A. Rahab¹, F. Senani², H. Benalla³

^{1,2,3} Laboratoire d'Electrotechnique de Constantine Université des Frères Mentouri Constantine1, Ain El-Bey 25000 Constantine, Algeria

Article Info

Article history:

Received Oct 30, 2016

Revised Jan 05, 2016

Accepted Jan 15, 2017

Keyword:

Wind turbine

BDFIG

Direct power control

MPPT

Wind energy conversion

ABSTRACT

This article describes firstly a wind power production line, principally a wind turbine constitutes her and brushless doubly fed induction generator (BDFIG). The models of these components are developed, and control objective of BDFIG is to achieve a dynamic performance similar to the doubly fed induction generator (DFIG) using a stator flux field oriented control (FOC) and direct power control (DPC) strategy. After, the simulation program using Matlab/Simulink has been developed. The performances of this strategy are evaluated and analyzed, so the results shows a good robustness great dynamic and a precision of speed.

Copyright © 2017 Institute of Advanced Engineering and Science.
All rights reserved.

Corresponding Author:

Rahab Abderezzak,
Laboratoire d'Electrotechnique (LEC),
Université des Frères Mentouri Constantine1,
Ain El-Bey 25000 Constantine, Algeria.
Email: rahababderezzak@gmail.com

1. INTRODUCTION

Wind power has become increasingly popular because of the increasing difficulty of the environmental pollution and the greenhouse effect. Huge efforts have been made in promoting the wind energy conversion system, to reduce costs, increase reliability and robustness [1]. The permanent magnet synchronous generator (PMSG) and the doubly fed induction generator (DFIG) have become the most popular generators for wind energy applications. On one hand, the use of brushes and slip rings associated with the rotor of DFIG decreases the robustness of system and increases the maintenance cost [2].

The cost of maintenance for traditional DFIG based windgenerators increased the pressure to seek other alternative generator systems. TheBrushless Doubly-Fed Induction Generator (BDFIG), also known as a self-cascaded generator, is composed of two stator of different pole numbers called stator of power winding (PW) and stator of control winding (CW) and a special rotor winding. Normally, the two stator supplies are of various frequencies, one a fixed frequency supply linked to the grid via converter, and the other a variable frequency supply derived from (AC-DC-AC) converter. The natural synchronous speed of the machine is equal to:

$$\omega_r = \frac{\omega_p + \omega_c}{P_p + P_c} \quad (1)$$

Where P_p , P_c , ω_p , ω_c and ω_r represents respectively, pole-pair of the PW, pole pair of CW, angular frequency of PW, angular frequency of CW and, Then the shaft angular speed.

The variable speed constant frequency (VSCF) generator system of the turbine is more important to improve the effectiveness in capturing the maximum energy of the wind and the assistance of the high quality, the efficiency and the power controllable, where the major challenge is the independent control of the active and reactive power exchanged between the BDFG and the grid.

A generator of a wind turbine should be fully controllable so that it can operate at a speed of shaft which is dependent on wind conditions to obtain the maximum output power. Furthermore, reactive power control is important for the production of electricity, and consequently, the functionality of the generator controller to regulate the power factor is essential. Because the BDFIG isn't stable over the complete running speed range, a controller is required to stabilize the machine at the same time as achieving nice dynamic overall performance in controlling the speed and reactive energy. Robustness and fast dynamic reaction are critical capabilities of such a controller for wind-electricity programs [3].

Some strategies of control have been used up to now in this machine (scalar current control, direct torque control, fuzzy power control, sliding mode power control, and the rotor flux oriented control. A new vector controller using a dynamic model with a unified reference frame based on the PW flux was investigated for the BDFM [4]. Furthermore simplified controller oriented with the PW stator flux with a complete mathematical derivation frame has been exhibited. with some experimental results presented on both speed and reactive power regulating [5].

Classical control strategies for grid side converter (GSC) systems regulate both the active power and reactive power flow by controlling the current vector orientation with respect to the grid voltage vector. This technique is referred to as voltage oriented control (VOC) [5],[6]. The VOC technique decomposes the AC line currents into the direct and quadrature components by using the Park transformation. This makes possible to regulate the active and reactive powers by controlling the decoupled AC currents, using current controllers [7].

However, there are a new strategies used to control grid- tied VSI systems in this type of program which include as the Direct Power Control (DPC). One of the fundamental qualities of the DPC is that the control directly the instantaneous active and reactive powers instead of instantaneous AC line currents. The DPC is mainly based on the principle of Direct Torque Control (DTC) for electrical machines [8]. In effect the DTC guides the stator flux and controls the torque of AC machines according to a switching table. Similarly, the DPC regulates instantaneous active and reactive powers by using an optimal switching table. This table determines the VSI switching states by means of using the errors of power and the position of the grid voltage vector.

This paper is dedicated to the study and control of the wind power system based on a BDFIG the use of indirect control power of machine side converter (MSC) by using PI controller and (DPC) control of (GSC) converter to control the voltage of the DC Link, MPPT method is carried out to extract the maximum power available. Figure 1 show the schematic diagram of power and control circuits of WECS studied in this paper.

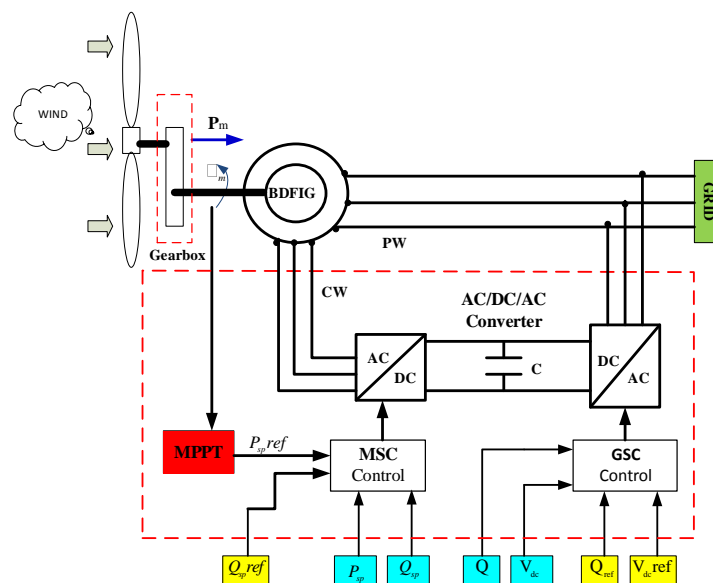


Figure 1. Schematic diagram of a BDFIG based wind power system

2. WECS MODELLING

2.1. Aerodynamic Model

The wind turbine is a device that converts kinetic energy of wind into mechanical energy. Wind power is defined as follows [9]:

$$P_v = \frac{1}{2} \pi \rho R^2 v^3 \tag{2}$$

The aerodynamic power (P_a) captured by the wind turbine is given by:

$$P_a = \frac{1}{2} \pi \rho R^2 C_p (\lambda, \beta) v^3 \tag{3}$$

The wind turbine is characterized by its curve $C_p=f(\lambda)$ [10]-[13].The tip speed ratio (λ) is expressed by the following expression :

$$\lambda = \frac{R\Omega_{tur}}{v} \tag{4}$$

C_p : power coefficient; ρ : density of air (1.25 Kg/m3);

v : wind speed; Ω_{tur} : wind turbine speed; R : turbine rayon.

The power coefficient C_p represents the aerodynamic efficiency of the wind turbine, it is determine by [10] :

$$C_p(l, b) = c_1(c_2 / l_i + c_3 b + c_4) e^{-c_5 / l_i} + c_6 l_i \tag{5}$$

Where,

$$\frac{1}{l_i} = \frac{1}{l + 0.08b} - \frac{0.035}{b^3 + 1} \tag{6}$$

With,

$c_1 = 0.51, c_2 = 116, c_3 = 0.5, c_4 = 5, c_5 = 21$ and $c_6 = 0.0068$.

Figure 2 show the typical curves of the power coefficient. We note that the maximum (C_{pmax}) is reached for: ($l = 8$ and $b = 0$).

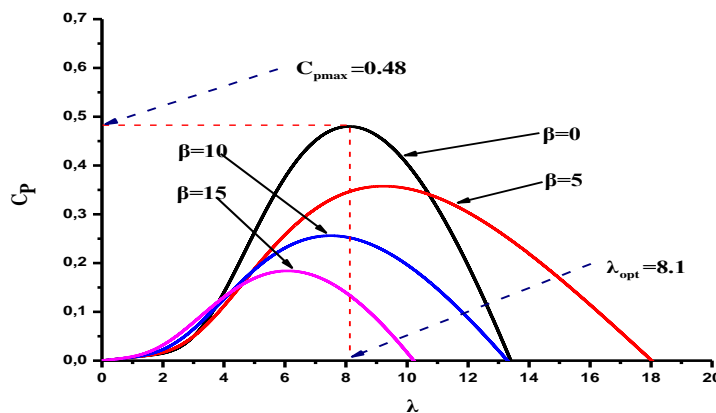


Figure 2. Typical curve of power coefficient

From this power the wind torque is given by:

$$C_a = \frac{P_a}{W_{tur}} = C_p \cdot \frac{r \cdot S \cdot v^3}{2} \cdot \frac{1}{W_{tur}} \quad (7)$$

The dynamics equation is :

$$J \cdot \frac{dW_{mec}}{dt} = C_{mec} \quad (8)$$

$$J = \frac{J_{tur}}{G^2} + J_g \quad (9)$$

With:

C_{mec} : Total mechanical torque applied to the rotor;
 J : is the total inertia that appears on the generator rotor.
 The mechanical torque:

$$C_{mec} = C_g - C_{em} - C_{vis} \quad (10)$$

2.2. BDFG model

The model of the brushless doubly fed induction generator in the PW synchronously rotating d-q reference frame is expressed as [14]-[16].

$$\begin{cases} v_{qsp} = R_{sp} i_{qsp} + \frac{d\Phi_{sp}}{dt} + \omega_p \Phi_{dsp} \\ v_{dsp} = R_{sp} i_{dsp} + \frac{d\Phi_{dsp}}{dt} - \omega_p \Phi_{qsp} \\ v_{dsc} = R_{sc} i_{dsc} + \frac{d\Phi_{dsc}}{dt} - (\omega_p - (p_p + p_c) \omega_r) \Phi_{qsc} \\ v_{qsc} = R_{sc} i_{qsc} + \frac{d\Phi_{qsc}}{dt} + (\omega_p - (p_p + p_c) \omega_r) \Phi_{dsc} \\ 0 = R_r i_{dr} + \frac{d\Phi_{dr}}{dt} - (\omega_p - p_p \omega_r) \Phi_{qr} \\ 0 = R_r i_{qr} + \frac{d\Phi_{qr}}{dt} + (\omega_p - p_p \omega_r) \Phi_{dr} \end{cases} \quad (11)$$

$$\begin{cases} \dot{\mathbf{F}}_{dsp} = \mathbf{L}_{sp} \dot{\mathbf{i}}_{dsp} + \mathbf{M}_{spr} \dot{\mathbf{i}}_{dr} \\ \dot{\mathbf{F}}_{qsp} = \mathbf{L}_{sp} \dot{\mathbf{i}}_{qsp} + \mathbf{M}_{spr} \dot{\mathbf{i}}_{qr} \\ \dot{\mathbf{F}}_{dsc} = \mathbf{L}_{sc} \dot{\mathbf{i}}_{dsc} + \mathbf{M}_{scr} \dot{\mathbf{i}}_{dr} \\ \dot{\mathbf{F}}_{qsc} = \mathbf{L}_{sc} \dot{\mathbf{i}}_{qsc} + \mathbf{L}_{scr} \dot{\mathbf{i}}_{qr} \\ \dot{\mathbf{F}}_{dr} = \mathbf{L}_r \dot{\mathbf{i}}_{dr} + \mathbf{M}_{scr} \dot{\mathbf{i}}_{dsc} + \mathbf{L}_{spr} \dot{\mathbf{i}}_{dsp} \\ \dot{\mathbf{F}}_{qr} = \mathbf{L}_r \dot{\mathbf{i}}_{qr} + \mathbf{M}_{scr} \dot{\mathbf{i}}_{qsc} + \mathbf{L}_{spr} \dot{\mathbf{i}}_{qsp} \end{cases} \quad (12)$$

The electromagnetic torque is expressed as [10] :

$$C_{em} = p_p \mathbf{M}_{spr} (i_{qsp} i_{dr} - i_{dsp} i_{qr}) + p_c \mathbf{M}_{scr} (i_{dsc} i_{qr} - i_{qsc} i_{dr}) \quad (13)$$

The active and reactive powers of the stator of PW are defined as:

$$P_p = \frac{3}{2}(V_{sdp} \cdot I_{sdp} + V_{sqp} \cdot I_{sqp}) \quad (14)$$

$$Q_p = \frac{3}{2}(V_{sqp} \cdot I_{sdp} - V_{sdp} \cdot I_{sqp}) \quad (15)$$

3. CONTROL STRATEGIES

3.1. Maximum Power Point Tracking Technique

It is evident that it is clear that the wind power is affected by the wind speed. The wind speed increases with the height most rapidly near the ground, increasing less rapidly with greater height. The wind speed at which electric power production starts called *the cut-in wind speed*. The turbine will develop enough mechanical power to rotate itself at slightly lower speeds, but this wind speed will actually supply all the generator and transmission losses so that useful electric power cannot be produced. At *rated wind speed* the power input to the wind turbine will reach the limit for continuous operation (rated power). When the wind speed exceeds this level the excess power in the wind must be discarded by varying the pitch angle of the blades to prevent the turbine overloading. The power is maintained at its rated value until a maximum wind speed is reached the *cut-off wind speed* ($V_{cut-off}$) then the turbine will shut down Figure 3 [13].

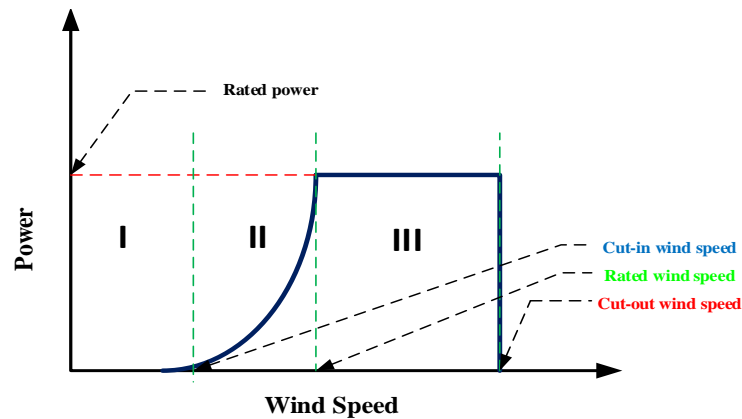


Figure 3. Wind turbine power curve characteristics

Maximum power point tracking (MPPT) strategies play an important role in wind power conversion systems (WECS) because they maximize the power extracted from the wind, and therefore optimize the conversion efficiency [17].

Figure 4 shows the Power-Speed characteristics of the wind turbine, the peak power for each wind speed occurs at the point where C_p is maximized. To maximize the power generated, it is therefore desirable for the generator to have a power characteristic that will follow the maximum C_{pmax} line.

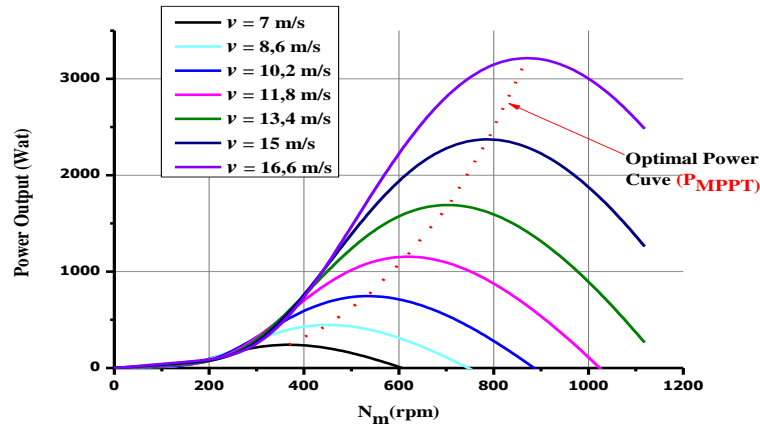


Figure 4. Characteristics curve of wind turbine

To extract the maximum power generated, we must maintain λ at the optimal command rotor speed λ_{opt} . The coordinates of the optimal point is the maximum power coefficient C_p are ($\lambda_{opt} = 8.1, C_{pmax} = 0.48, \beta = 0$). Increasing β allows the reduction of mechanical power recovered from the axis of the wind turbine (see Figure 4).

Two strategies are used in literature [18], with or without speed control. In this paper, we used the strategy with speed control; it permits to conduct the speed wind turbine to the desired value which corresponds to the maximum power point. The simplified representation of wind turbine model with speed control in the form of diagram blocks is given in Figure 5.

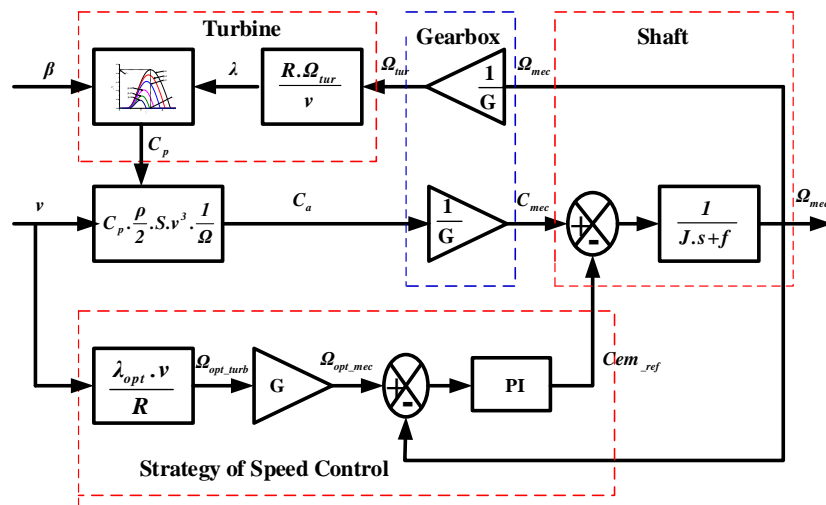


Figure 5 Wind turbine model with speed control

3.2. Control of the BDFG with a PW field oriented

If the d-axis of the PW synchronous reference frame is aligned with the PW air gap flux, the R_p of PW is neglected. Then, the relation between the PW voltage and its flux is:

$$\begin{cases} \dot{V}_{dsp} = 0 \\ \dot{V}_{qsp} = V_p = \omega_p \cdot F_p \end{cases} \tag{16}$$

$$\begin{cases} F_{dsp} = L_{sp} i_{dsp} + M_{spr} i_{dr} \\ 0 = L_{sp} i_{qsp} + M_{spr} i_{qr} \end{cases} \quad (17)$$

From (17), the equations linking the rotor currents to the PW currents are deduced as:

$$\begin{cases} i_{dr} = \frac{F_p}{M_{spr}} - \frac{L_{sp}}{M_{spr}} i_{dsp} \\ i_{qr} = -\frac{L_{sp}}{M_{spr}} i_{qsp} \end{cases} \quad (18)$$

Figure 6 shows the control algorithm of BDFIG

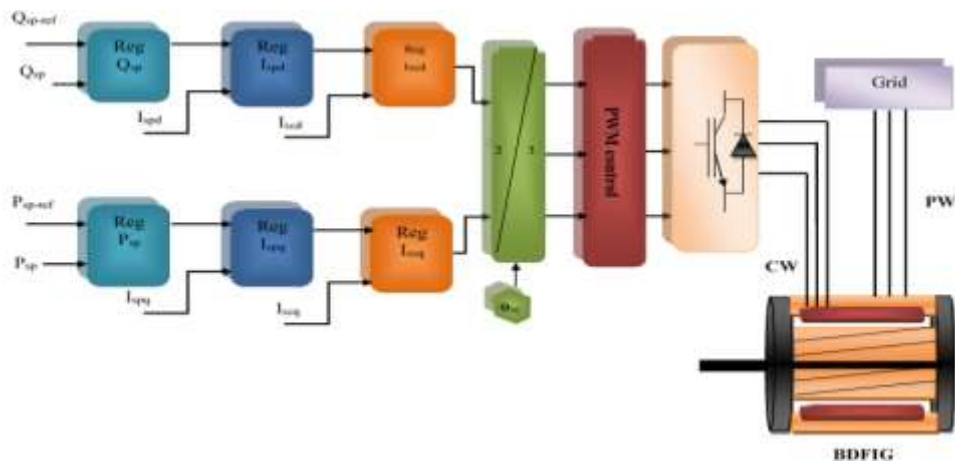


Figure 6. General Scheme control of BDFIG

This scheme is based on the cascade regulation method [4]. Two independent regulation paths are implemented:

Reactive power control: $Q_{sp} \textcircled{R} i_{spd} \textcircled{R} i_{scd} \textcircled{R} V_{scd}$

Active power control: $P_{sp} \textcircled{R} i_{spq} \textcircled{R} i_{scq} \textcircled{R} V_{scq}$

3.3. PW current Control

The current derivative (CW) is given by the equation:

$$\frac{di_{scd}}{dt} = \frac{R_{sp} L_{sp}}{M_{spr} M_{scr}} i_{scd} - \frac{L_{sp} L_r S_{sp}}{M_{spr} M_{scr}} \frac{di_{scd}}{dt} - \frac{R_r}{M_{scr} M_{scr}} |F_{sp}| - w_{Rsp} \frac{L_{sp} L_r S_{sp}}{M_{spr} M_{scr}} i_{scq} + w_{Rsp} i_{sp}^q \quad (19)$$

$$\frac{di_{scq}}{dt} = \frac{R_{sp} L_{sp}}{M_{spr} M_{scr}} i_{scq} - \frac{L_{sp} L_r S_{sp}}{M_{spr} M_{scr}} \frac{di_{scq}}{dt} - \frac{R_r}{M_{spr} M_{scr}} |F_{sp}| - w_{Rsp} \frac{L_{sp} L_r S_{sp}}{M_{spr}} i_{spq} + w_{Rsp} i_{scq} \quad (20)$$

Relationships (19) and (20) can be rearranged into two terms:

$$\begin{cases} \frac{di_{scd}}{dt} = a_{xd} i_{spd} + a_{yd} (i_{spq}, i_{scq}, |F_{sp}|) \\ \frac{di_{scq}}{dt} = a_{xq} i_{spq} + a_{yq} (i_{spd}, i_{scd}, |F_{sp}|) \end{cases} \quad (21)$$

With :

$$\begin{cases} \dot{a}_{xd} = \frac{R_{sp} L_{sp}}{M_{spr} M_{spr}} \cdot i_{spd} - \frac{L_{sp} L_r s_{sp}}{M_{spr} M_{scr}} \frac{di_{spd}}{dt} \\ \dot{a}_{yd} = - \frac{R_r}{M_{spr} M_{scr}} \left| \mathbf{F}_{sp} \right| - w_{Rsp} \frac{L_{sp} L_r s_{sp}}{M_{spr} M_{scr}} i_{spq} + w_{Rsp} i_{scq} \end{cases} \quad (22)$$

$$\begin{cases} \dot{a}_{xq} = \frac{R_{sp} L_{sp}}{M_{spr} M_{s2r}} \cdot i_{spq} - \frac{L_{sp} L_r s_{sp}}{M_{spr} M_{scr}} \cdot \frac{di_{spq}}{dt} \\ \dot{a}_{yq} = - \frac{R_r}{M_{spr} M_{scr}} \cdot \left| \mathbf{F}_{sp} \right| - w_{Rsp} \frac{L_{sp} L_r s_{sp}}{M_{spr}} \cdot i_{spq} + w_{Rsp} i_{scq} \end{cases} \quad (23)$$

The $a_{xd}(i_{spd})$ and $a_{xq}(i_{spq})$ reflect a linear relationship between direct current vector components of (PW) and (CW), while $a_{yd}(i_{spq}, i_{scq}, \left| \mathbf{F}_{sp} \right|)$ and $a_{yq}(i_{spq}, i_{scd}, i_{scq}, \left| \mathbf{F}_{sp} \right|)$ represent the current coupling between the cross vector components d and q.

3.4. CW current control

The current derivative (PW) is given by the equation:

$$\frac{di_{spd}}{dt} = \frac{M_{spr} M_{scr}}{L_{sp} L_r s_{sp}} \left(M_{scr} \cdot \frac{di_{scd}}{dt} - \frac{L_{sp} R_r}{M_{spr}} i_{spd} + \frac{R_r}{M_{spr}} \left| \mathbf{F}_{sp} \right| \right) + \frac{M_{spr} M_{scr}}{L_p L_r s_{sp}} \cdot (w_{Rsp} L_{sp} s_{sp} i_{spq} - w_{Rsp} M_{scr} i_{scq}) \quad (24)$$

$$\frac{di_{spq}}{dt} = \frac{M_{spr} M_{scr}}{L_{sp} L_r s_{sp}} \left(M_{scr} \cdot \frac{di_{scq}}{dt} - \frac{L_{sp} R_r}{M_{spr}} i_{spq} + \frac{R_r}{M_{spr}} \left| \mathbf{j}_{sp} \right| \right) + \frac{M_{spr} M_{scr}}{L_{sp} L_r s_{sp}} \cdot (-w_{Rsp} L_{sp} s_{sp} i_{spd} + w_{Rsp} M_{scr} i_{scd}) \quad (25)$$

The tension of (CW) given by the equation:

$$\begin{cases} v_{scd} = b_{xd} \cdot i_{spd} + b_{yd} (i_{spd}, i_{spq}, i_{scq}, \left| \mathbf{F}_{sp} \right|) \\ v_{scq} = b_{xq} \cdot i_{spq} + b_{yq} (i_{spd}, i_{spq}, id, \left| \mathbf{F}_{sp} \right|) \end{cases} \quad (26)$$

whose individual terms are:

$$\begin{cases} b_{xd} = R_{sp} i_{scd} + \left(L_{sc} - \frac{M_{scr}^2}{L_r s_{sp}} \right) \frac{di_{scd}}{dt} \\ b_{yd} = \frac{M_{spr} M_{scr} R_r}{L_{sp} L_r s_{sp}} i_{spd} - \frac{M_{scr} R_r}{L_{sp} L_r s_{sp}} \left| \mathbf{j}_{sp} \right| - p_p w_r \frac{M_{scr} L_{sp}}{M_{spr}} i_{spq} + \frac{\dot{M}_{scr}^2}{L_r s_{sp}} w_{Rsp} - (w_{Rsp} - p_c w_r) L_{sc} \frac{\dot{u}}{u} i_{scq} \end{cases} \quad (27)$$

$$\begin{cases} b_{xq} = R_{sp} i_{scq} + \left(L_{sc} - \frac{M_{scr}^2}{L_r s_{sp}} \right) \frac{di_{scq}}{dt} \\ b_{yq} = \frac{M_{spr} M_{scr} R_r}{L_{sp} L_r s_{sp}} i_{spq} - \frac{M_{scr} \dot{M}_{scr}}{M_{spr} L_r s_{sp}} - 1 \cdot p_p w_{Rsp} \frac{\dot{u}}{u} \left| \mathbf{j}_{sp} \right| + p_p w_r \frac{M_{scr} L_{sp}}{M_{scr}} i_{spq} + \frac{\dot{M}_{scr}^2}{L_r s_{sp}} w_{Rsp} - (w_{Rsp} - p_c w_r) L_{sc} \frac{\dot{u}}{u} i_{scd} \end{cases} \quad (28)$$

3.5. Active and reactive power Control

The expression of reactive power based on the flow and current is:

$$Q_{sp} = \frac{3}{2} \cdot w_{sp} \left| \mathbf{F}_{sp} \right| \cdot i_{spd} - \frac{d \left| \mathbf{F}_{sp} \right|}{dt} \cdot i_{spq} \quad (29)$$

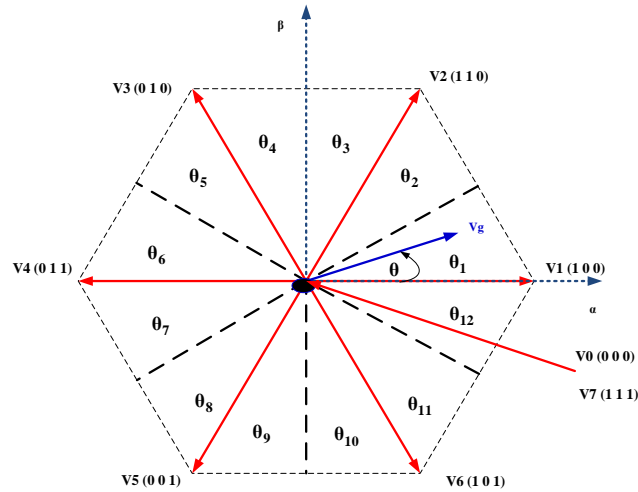


Figure 8. Twelve (12) sectors on stationary coordinates to specify voltage vector phase

For this purpose, the stationary coordinates are divided into 12 sectors, as shown in Figure 8, and the sectors can be numerically expressed as:

$$(n-2) \cdot \frac{P}{6} \leq q_n \leq (n-1) \cdot \frac{P}{6}; n = 1, 2, 3, \dots, 12 \tag{33}$$

$$d_p = \begin{cases} 1 & \text{for } P \leq P_{ref} - H_p \\ 0 & \text{for } P > P_{ref} - H_p \end{cases} \tag{34}$$

Similarly for reactive power controller:

$$d_q = \begin{cases} 1 & \text{for } Q \leq Q_{ref} - H_q \\ 0 & \text{for } Q > Q_{ref} - H_q \end{cases} \tag{35}$$

With, d_p, d_q are digitized error signals of P and Q ; θ_n : voltage phase; ($S_a, S_b,$ and S_c): switching state.

Table 1. Switching Table for DPC

d_p	d_q	$\theta 1$	$\theta 2$	$\theta 3$	$\theta 4$	$\theta 5$	$\theta 6$	$\theta 7$	$\theta 8$	$\theta 9$	$\theta 10$	$\theta 11$	$\theta 12$
1	0	101	111	100	000	110	111	010	000	011	111	001	000
1	1	111	111	000	000	111	111	000	000	111	111	000	000
0	0	101	100	100	110	110	010	010	011	011	001	001	101
0	1	100	110	110	010	010	011	011	001	001	101	101	100

The instantaneous input active and reactive powers of three phase rectifier are generally defined as:

$$P = e_a \cdot i_a + e_b \cdot i_b + e_c \cdot i_c \tag{36}$$

$$Q = \frac{1}{\sqrt{3}} [(e_b - e_c) i_a + (e_c - e_a) i_b + (e_a - e_b) i_c] \tag{37}$$

$$q = \arctan \left(\frac{e_b \frac{d}{dt} i_c - e_c \frac{d}{dt} i_b}{e_a \frac{d}{dt} i_c} \right) \tag{38}$$

4. SIMULATION RESULTS

The simulation was performed with the Matlab / Simulink software to validate the commands studied in this work. We realized two operating points, one on the step of speed (see Figure 9(a)) and other variable speed (see wind profil Figure 16(a)). The wind speed is modelled by deterministic form a sum of several harmonics:

$$V_{wind} = V_0 + \sum_{i=0}^n V_i \sin(\omega_i t) \quad (39)$$

The parameters of BDFIG used of this study are given in Table 1.

Table 3. BDFIG Parametres [4]

Power Windin (PW)	Control Windin(CW)	Rotor
$R_{sp} = 1.732 \text{ W}$	$R_{sc} = 1.079 \text{ W}$	$R_r = 0.473 \text{ W}$
$L_{sp} = 714.8 \text{ mH}$	$L_{sc} = 121.7 \text{ mH}$	$L_r = 132.6 \text{ mH}$
$M_{spr} = 242.1 \text{ mH}$	$M_{spr} = 59.8 \text{ mH}$	$f_p = 50 \text{ Hz}$
$P_p = 1$	$P_c = 3$	
$L_r = 142 \text{ mH}$	$r_r = 1.65 \text{ } \Omega$	

Concerning the results of the simulations, two cases have been analyzed corresponding to the profiles of wind respectively represented, by the Figures 9(a) and 16(a). However for the two (2) profiles :

The speeds (see Figures 9(b) and 16(b)) are almost adapted to the wind speed, respectively, resulting in a very significant increase of the power. By elsewhere, the speed is less than that of the synchrony (750 tr/m). This technique of extraction of the maximum of power is to determine the speed of the turbine which allows you to get the maximum of power generated. Also, we note that the amplitudes of the current of phases as the winding of power and control (Figures 10(a), 11(a), 17(a) and 18(a)), consequent change, with the variation of the speed of the wind and that their forms sinusoidal are given by the figures (10(b), 11(b), 17(b) and 18(b)).

First According to the Figures(12(a), 19(a)) and their zoom illustrat by 12(b) and 19(b), respectively, it may be noted the robustness of the vector command in term of decoupling and the good results obtained by the regulation the active and reactive power, second, we show that a small variation of the wind can induce a large variation in the power extracted (mechanical power), because of the proportionality of this last to the average value of the cubic speed of the wind.

We distinguishes the sinusoidal shape of the current of phase of the PW and the reactive power is zero, which translated the production of electrical energy under unit power factor.

The MPPT strategy we allows to provide the totality of the active power produced at the electrical network with a unit power factor. However, the command decoupled from the active and reactive power allows to regulate the active and reactive power provided to the network. Figures 13 and 20 shows the CW current components i_{dc} and i_{qc} . This components imposent, respectivement, the reactive power (Q) and active power (P).

The component in squaring of the flow (fluxqp) of (PW) cancels in permanent regime, and the direct component of the flow (PW) (fluxdp) is equal to the value (-1.1 Wb) (see Figure 14 and 21), and the brusque variation of the active power (Psp) has no influence on the flow of (PW). The Figures 14 shows the flow of BP, one distinguishes the orientation of the flow on the direct axis, such as $\text{fluxdp} = 0$, this justifies that the command to flow oriented.

The variation of the electrical power delivered to the network is adapted to the variation consequence of the speed of the BDFIG, and the latter is adapted to the variation in the wind speed of the wind. This shows the influence of the variation of the mechanical speed as a function of the speed of the wind on the electrical power produced.

It was also noted that the simulation results show a continued good set point for the stator currents (PW) and (CW). The instructions of power are well followed by the generator as well for the active power that for the reactive power which is maintained zero. The stator frequency of the machine (control winding) depends on the speed of rotation of the turbine.

Figures 15 and 20 shows that the voltage of continuous bus (Vdc) stabilizes on its reference value (600 V) imposed by the command, and The continuing tension in output of the rectifier is well controlled and quasi-insensitive to variations in the speed.

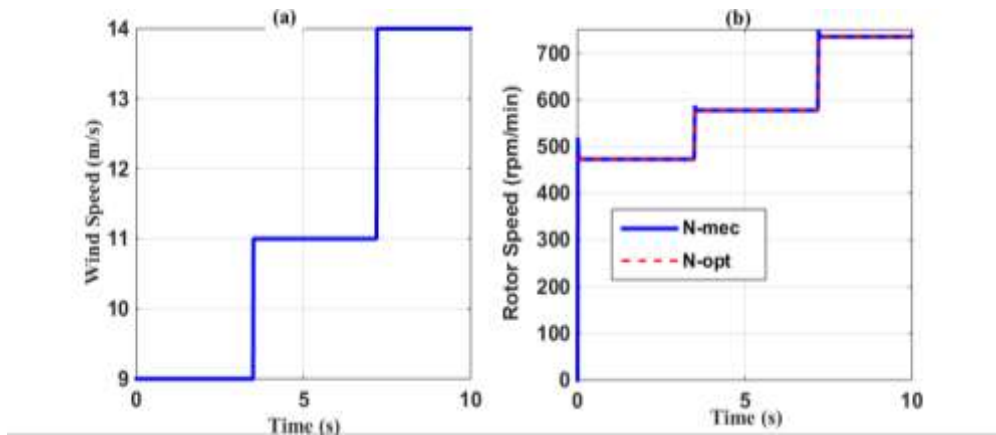


Figure 9. Wind Speed, Rotor Speed

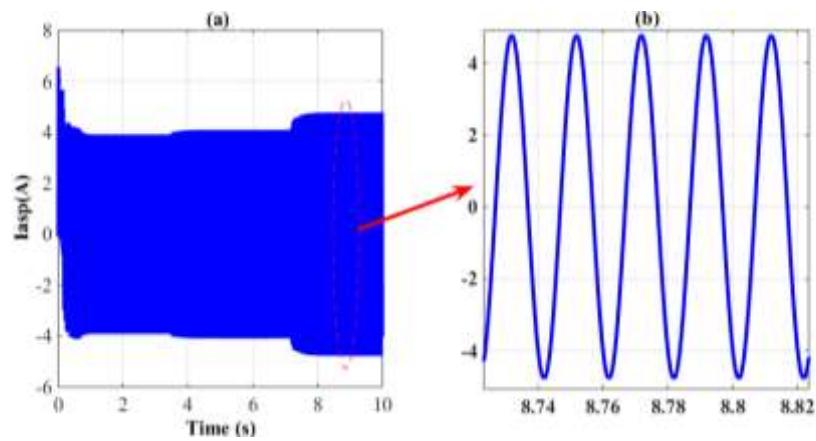


Figure 10. Phase PW current of phase-a and zoom

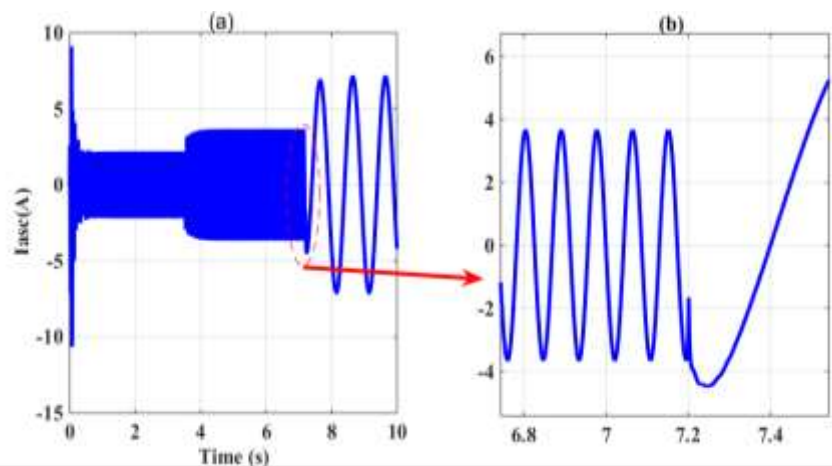


Figure 11. Phase CW current of phase -a and zoom

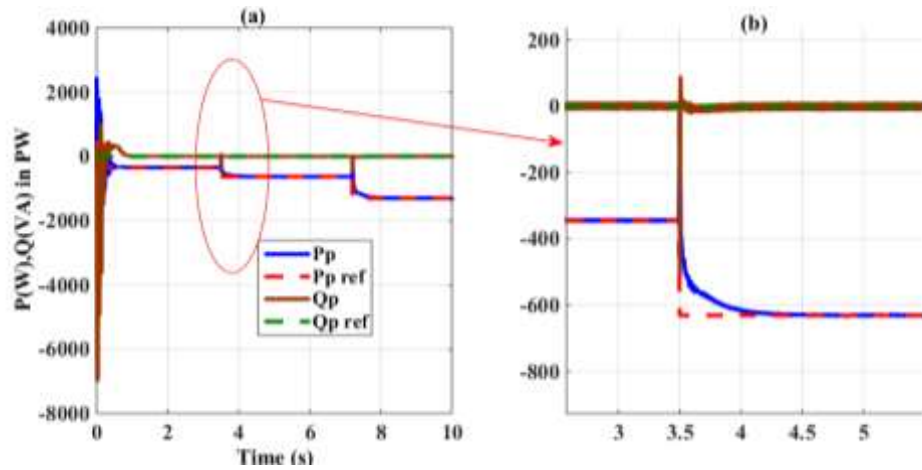


Figure 12. Power of PW

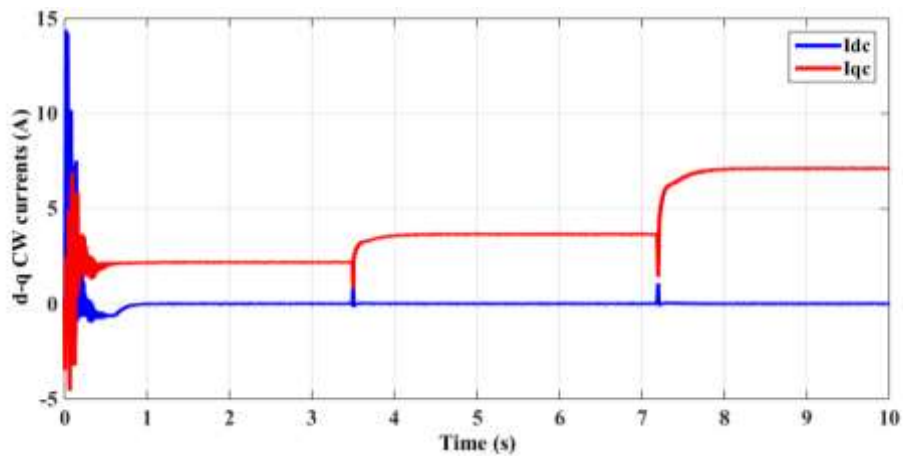


Figure 13. d-q CW Current

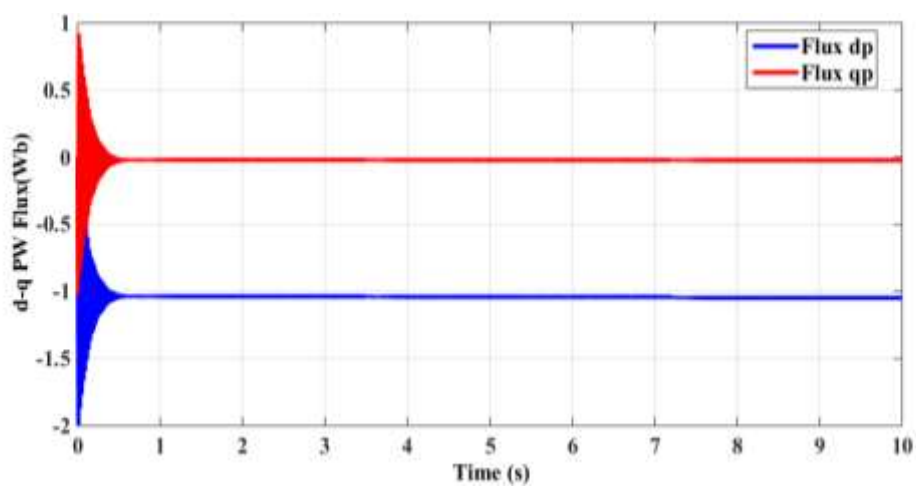


Figure 14. d-q PW Flux

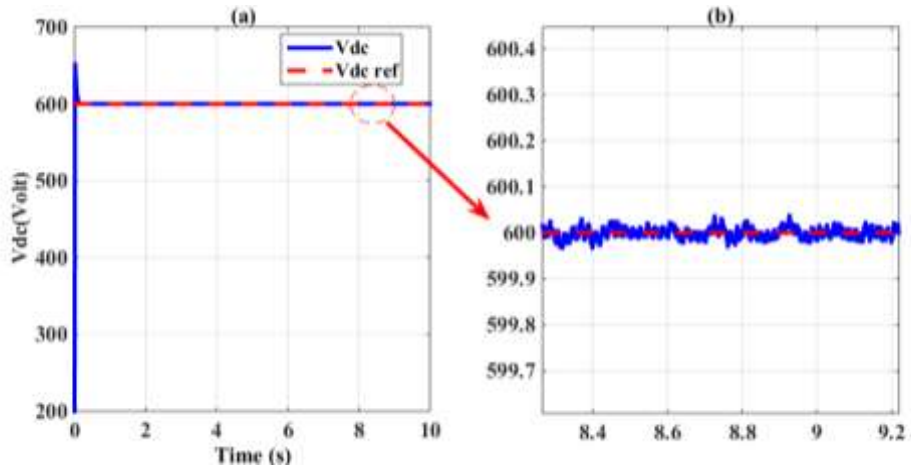


Figure 15. DC link Voltage

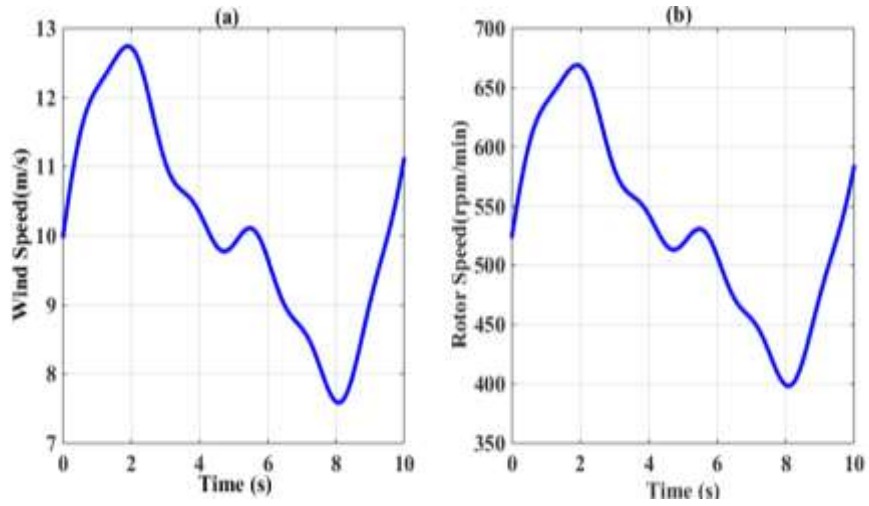


Figure 16. Wind Speed, Rotor Speed

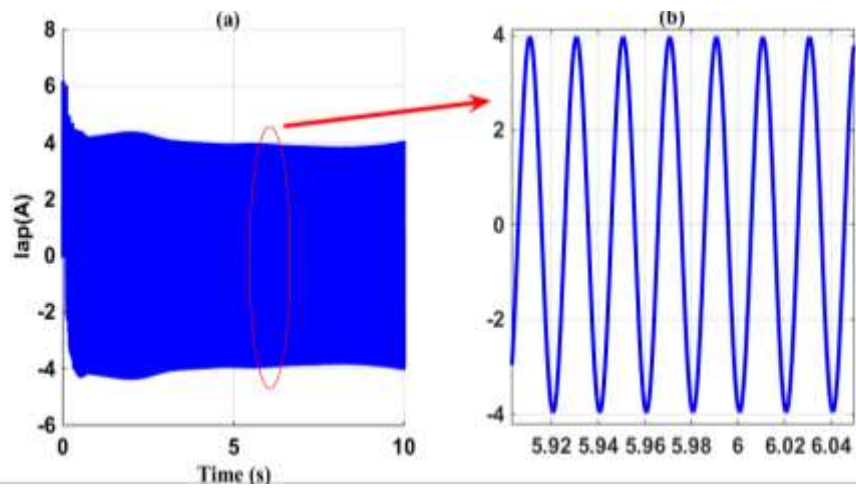


Figure 17. Phase PW current

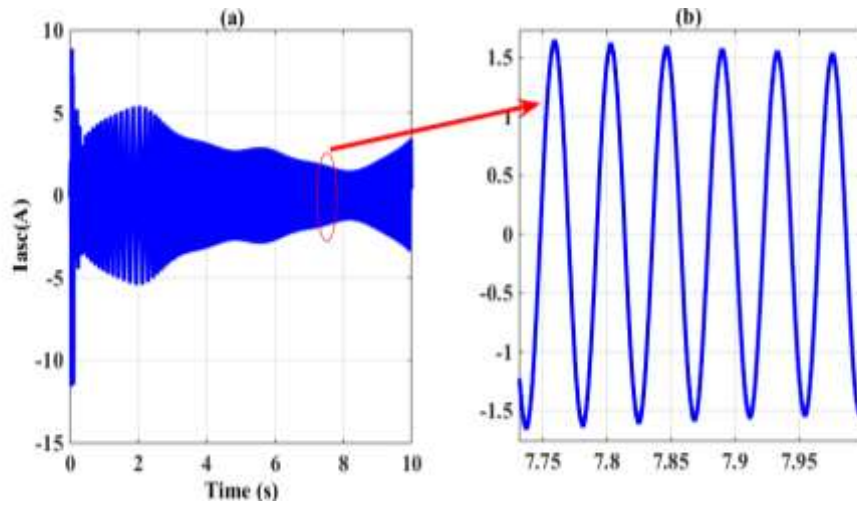


Figure 18. Phase CW current

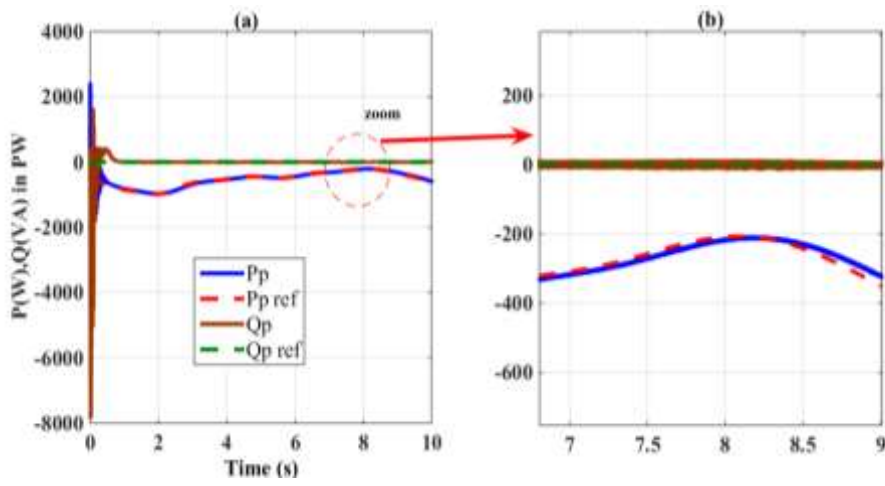


Figure 19. Power of PW

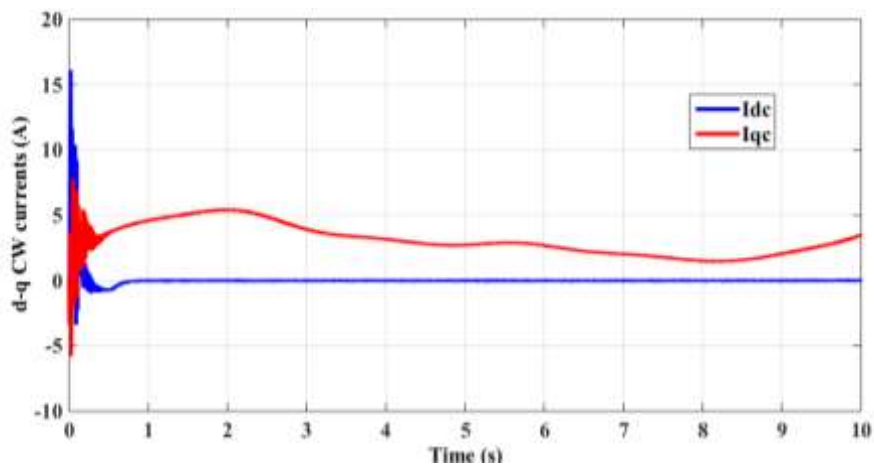


Figure 20. d-q CW Currents

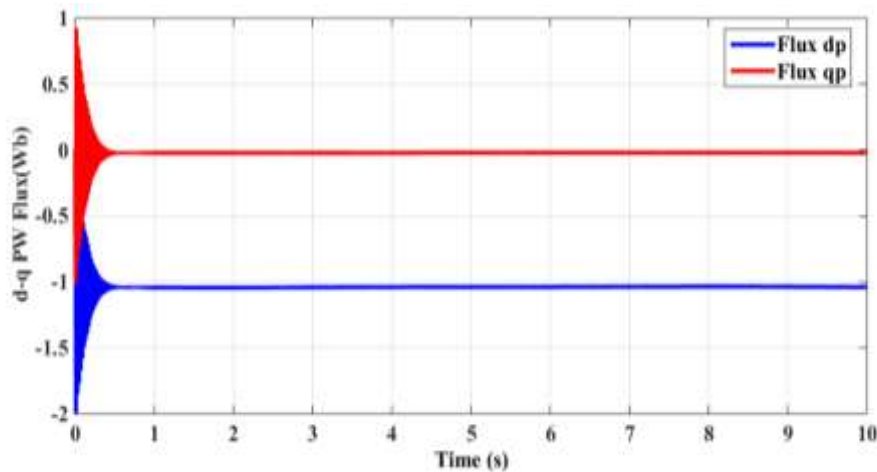


Figure 21. d-q PW Flux

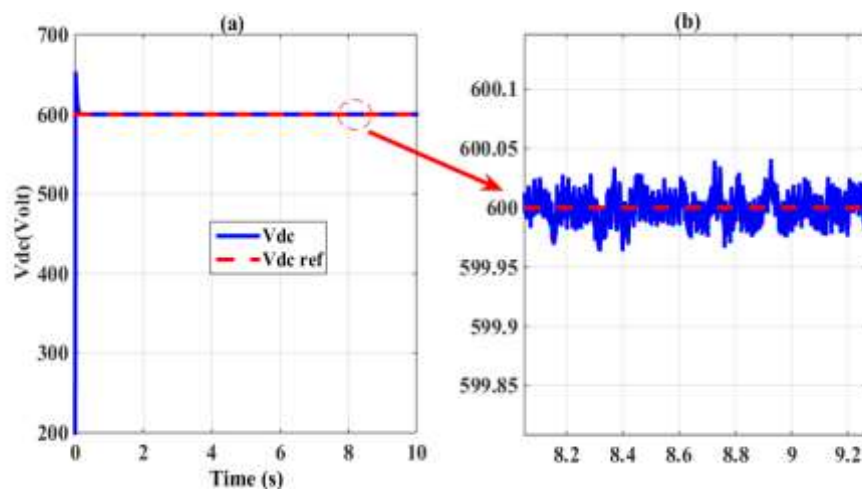


Figure 22. DC link Voltage

5. CONCLUSION

This work dealt with the modelling and control of a wind system with variable speed based on a brushless doubly fed induction generator. First, we have interested in modeling various parts of the wind turbine system, in order to establish the various controls on the two converters (MSC and GSC). The PW flux vector control is oriented to apply independent control of active power and reactive. Direct power control applied to the GSC converter to maintain constant DC link voltage and the technique of MPPT is applied to provide all of the active power generated to the grid with unity power factor. The results showed that the active and reactive power of the wind energy system could be controlled independently while ensuring optimum active power supplied to the grid, DPC applied to the GSC provides excellent dynamic response and good steady state performances. The results of the simulation show that performance system is encouraging.

REFERENCES

- [1] M. Cheng and Y. Zhu, "The state of the art of wind energy conversionsystems and technologies: A review," *Energy Convers. Manage*, vol. 88, pp. 332-347, 2014.
- [2] M. Cheng, *et al.*, "Modeling and control of a novel dual-stator brushless doubly-fed wind power generation system," in *Proc. Int. Conf. Elect. Mach. Syst.*, pp. 3029-3035, 2014.
- [3] S. Shao, *et al.*, "Stator-Flux-Oriented Vector Control for Brushless Doubly Fed Induction Generato," *IEEE Transactions on Industrial Electronics*, vol/issue: 56(10), pp. 4220-4228, 2009.

- [4] J. Poza, *et al.*, "Vector control design and experimental evaluation for the brushless doubly fed machine," *IET Electr. Power Appl.*, vol/issue: 3(4), pp. 247-256, 2009.
- [5] N. Mendoza, *et al.*, "A Comparative Analysis of Direct Power Control Algorithms for Three-Phase Power Inverters," *Power and Energy Society General Meeting (PES)*, pp. 1-5, 2013.
- [6] M. Allagui, *et al.*, "A 2MW direct drive wind turbine vector control and direct torque control techniques comparison," *J. energy South. Afr.*, vol/issue: 25(2), pp. 117-126, 2014.
- [7] J. Hu, *et al.*, "Direct Active and Reactive Power Regulation of Grid-Connected DC/AC Converters Using Sliding Mode Control Approach," *IEEE Transactions on Power Electronics*, vol/issue: 26(1), pp. 210-222, 2011.
- [8] I. Takahashi and T. Noguchi, "A new quick response and high-efficiency control strategy of an induction motor," *IEEE Transactions on Industry Applications*, vol/issue: 22(5), pp. 820-827, 1986.
- [9] S. Heier, "Grid Integration of Wind Energy Conversion Systems," John Wiley & Sons Ltd., 1998.
- [10] F. Valenciaga, *et al.*, "Power Control of a Solar/Wind Generation System Without Wind Measurement: A Passivity/Sliding Mode Approach," *IEEE Transactions on Energy Conversion*, vol/issue: 18(4), pp. 501-507, 2003.
- [11] E. Koutroulis and K. Kalaitzakis, "Design of a maximum power tracking system for wind-energy-conversion Applications," *IEEE Transactions on Industrial Electronics*, vol/issue: 53(2), pp. 486-494, 2006.
- [12] T. Khalfallah, *et al.*, "Power Control of Wind Turbine Based on Fuzzy Sliding-Mode Control," *International Journal of Power Electronics and Drive System (IJPEDS)*, vol/issue: 5(4), pp. 502-511, 2015.
- [13] Y. Mastanamma and S. Deepthi, "Harmonic Analysis of Doubly Fed Induction Generator for Wind Energy Conversion Systems Using MATLAB/Simulink," *International Journal of Advanced Research in Electrical, Electronics and Instrumentation Engineering*, vol/issue: 4(5), pp. 4409-4414, 2015.
- [14] I. Sarasola, *et al.*, "Direct torque control design and experimental evaluation for the brushless doubly fed machine," *Energy Conversion and Management*, vol. 52, pp. 1226-1234, 2011.
- [15] P. C. Roberts, *et al.*, "Equivalent circuit for the brushless doubly fed machine (BDFM) including parameter estimation and experimental verification," *IEE Proc. Electr. Power*, vol/issue: 152(4), pp. 933 – 942, 2005.
- [16] D. Zhou and R. Spee, "Synchronous frame model and decoupled control development for doubly-fed machines," *Proc. IEEE PESC Conf.*, pp. 1129 –1236, 1994.
- [17] S. Kouadria, *et al.*, "Sliding mode control of the active and reactive power of DFIG for variable-speed wind energy conversion system," *3rd International Renewable and Sustainable Energy Conference (IRSEC)*, pp. 1-8, 2015.
- [18] Soliman, *et al.*, "Multiple model predictive control for wind turbines with doubly fed induction generators," *IEEE Trans. Sustain. Energy*, vol/issue: 25(3), pp. 215–225, 2011.
- [19] A. Razali, *et al.*, "Analysis and Design of New Switching Lookup Table for Virtual Flux Direct Power Control of Grid-Connected Three-Phase PWM AC–DC Converter," *IEEE Transactions on Industry Applications*, vol/issue: 51(2), pp. 1189 -1200, 2015.
- [20] N. Goel, *et al.*, "A Review of the DTC Controller and Estimation of Stator Resistance in IM Drives," *International Journal of Power Electronics and Drive System (IJPEDS)*, vol/issue: 6(3), pp. 554-566, 2015.
- [21] M. S. Djebbar and H. Benalla, "Performance and High Robustness DPC for PWM Rectifier under Unstable Direct Voltage Bus," *International Journal of Power Electronics and Drive System (IJPEDS)*, vol/issue: 7(1), pp. 66-74, 2016.